

$\lambda, \text{ \AA}$	$\nu, \text{ cm}^{-1}$	Proposed band of the $E'\Sigma_g^+ \rightarrow B'\Sigma_u^+$ system
8 335	11 998	2→1
8 879	11 263	
8 892	11 246	1→0
11 147	8 971	
11 205	8 925	0→0
13 100	7 634	
		0→1

it possible to obtain laser action at only one or two of these lines.

The observed laser lines may, within the accuracy of the measurements, be ascribed to transitions in the band system  $E'\Sigma_g^+ \rightarrow B'\Sigma_u^+$  of the hydrogen molecule. The band to which each line is assigned is shown in the table. In all cases the observed lines may be attributed to transitions belonging to the P-branch of the band; the rotational quantum number  $J$  does not exceed 4. Insufficient resolving power in the instrument with which we worked prevents us at present from more definite assignment of the observed lines to particular transitions.

All of the experimental results are consistent with the following mechanism for producing inversion. The equilibrium internuclear separations for the states of the hydrogen molecule under consideration are appreciably different. However the shape of the potential energy curves is such<sup>[1,2]</sup> that, according to the Franck-Condon principle, in a discharge one will preferentially populate relatively high vibrational levels of the state  $B'\Sigma_u^+$  with  $v'' = 5, 6, 7, 8, 9$ . The vibrational levels with smaller  $v''$  must be relatively less populated. On the other hand the population of the state  $E'\Sigma_g^+$  is in the lower vibrational levels  $v' = 0, 1, 2, 3$ . Moreover the shape of the potential curves is such that there must be relatively large probabilities for the transitions  $E'\Sigma_g^+ (v' = 0, 1, 2, 3) \rightarrow B'\Sigma_u^+ (v'' = 0, 1, 2)$ . Hence one would expect these transitions to be inverted, at least during the initial moments of the discharge when the level populations are determined primarily by electronic excitation from the ground state.

It can be expected that such a mechanism for producing inversion would have wide application for producing laser action in molecular electronic vibrational-rotational transitions.

<sup>1</sup>J. Tobias and J. T. Vanderslice, *J. Chem. Phys.* **35**, 1852 (1961).

<sup>2</sup>W. Kolos and C. C. J. Roothaan, *Revs. Modern Phys.* **32**, 219 (1960).

Translated by J. A. Armstrong  
222

## COMPTON EFFECT ON MOVING ELECTRONS

O. F. KULIKOV, Yu. Ya. TEL'NOV, E. I. FILIPPOV, and M. N. YAKIMENKO

Moscow State University; P. N. Lebedev  
Physics Institute, Academy of Sciences,  
U.S.S.R.

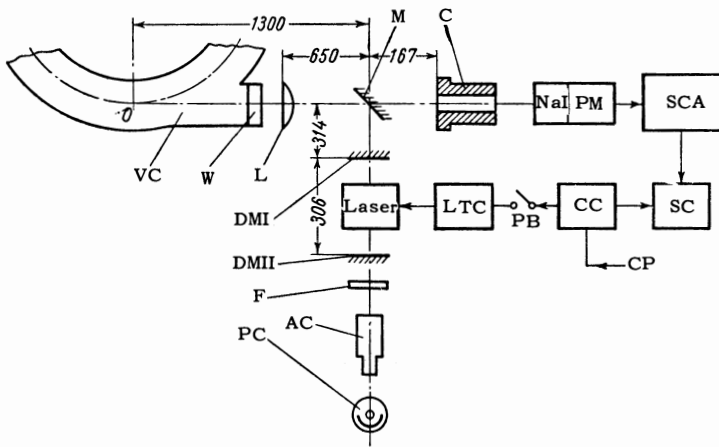
Submitted to JETP editor June 24, 1964

*J. Exptl. Theoret. Phys. (U.S.S.R.)* **47**, 1591-1594 (October, 1964)

UP to the present time the Compton effect has been studied experimentally for stationary (non-relativistic) electrons. With the development of methods of accelerating elementary particles, in particular electrons, the possibility has appeared of investigating the scattering of photons by electrons moving almost with the speed of light. The creation of new powerful photon sources - lasers - permits us to achieve the scattering of photons of visible light by electrons moving in the orbit of a cyclic accelerator.

The theory of the Compton effect on relativistic electrons, described by Akhiezer and Berestetskii,<sup>[1]</sup> has been discussed in detail for the case of interaction of laser photons with relativistic electrons by Milburn,<sup>[2]</sup> Arutyunyan and Tumanyan,<sup>[3]</sup> and Arutyunyan et al.<sup>[4]</sup> According to these theoretical treatments, for a head-on collision of laser radiation ( $\lambda = 6943 \text{ \AA}$ ) and relativistic electrons with an energy of the order of 500 MeV, we should expect the appearance of  $\gamma$  rays of energy about 7 MeV in the direction of motion of the electrons.

Since this effect can be very important in the study of the bunching of accelerated electrons and since the scattered  $\gamma$  rays can be utilized in various nuclear investigations, we have attempted to detect the scattered  $\gamma$  radiation arising in the interaction of colliding beams of photons from a ruby laser and electrons accelerated in the FIAN 600 MeV synchrotron. A diagram of the equipment is shown in the figure. The laser light is directed by the mirror M along a tangent to the electron orbit O in the accelerator vacuum chamber VC, in a direction opposite to the accelerated electrons. The  $\gamma$ -rays resulting from the scattering move along the same tangent to the electron orbit but in the opposite direction to the laser photons. Passing through the mirror M, they are incident on a scintillation counter with a NaI crystal. The signal from the photo-multiplier is fed through the amplifier and single-channel analyzer SCA to the



VC – vacuum chamber, O – orbit, W – glass window, L – lens, M – adjustable mirror, C – collimator, SCA – amplifier and single-channel analyzer, CS – scaling circuit, CP – control pulse, CC – control circuit, PB – push button switch, LTC – laser trigger circuit, DMI – laser mirror, DMII – laser mirror, F – optical filter, AC – auto collimation tube, PC – photocell.

scaling circuit SC, which is turned on by a special means. The scaling circuit operation is synchronized with the laser in such a way that the scaling circuit records  $\gamma$ -rays with a delay of 70  $\mu\text{sec}$  after the laser pumping tube trigger pulse, which corresponds to the beginning of the laser light, and operates for 620  $\mu\text{sec}$  during the flash of laser light. The triggering of the pumping tube is synchronized with the accelerator magnetic field and can be accomplished at any instant of the synchrotron magnetic cycle, i.e., at any energy of the accelerated electrons. During the laser light flash the energy of the electrons changes by less than 1 MeV. The acceleration cycles are repeated with a frequency of 0.16 cps. The laser light flash occurs at the appropriate instant of the next cycle after closing of the push-button switch PB. If the switch PB is not closed, the scaling circuit records the background from the accelerator.

Light from a 120 mm ruby crystal passes through the laser dielectric mirror DMI (transmission 17%) and the mirror M, and is focused on the electron orbit by the lens L (focal length 800 mm) through the glass window W of the synchrotron vacuum chamber tangent pipe. The diameter of the laser light spot at the electron orbit is  $\sim 3$  mm. The part of the laser light emerging from the opposite end of the ruby passes through the laser dielectric mirror DMII (transmission 4%) and the optical filter F, and is incident on the auto-collimation tube AC, which is used for adjustment of the laser. Beyond the ocular of the auto-collimation tube is located a photocell PC whose signal amplitude indicates the laser light yield. The scattered  $\gamma$  rays pass through the glass window W, the lens L, the mirror M, and collimator C (15 mm diameter), and produce a scintillation in the NaI crystal which is recorded by the photomultiplier. All dimensions in the diagram are given in mm. On the basis of the experimental geometry,

the effective segment of the electron orbit has a length of the order of 18 mm. Alignment of the collimator and the laser with the electron beam is accomplished by means of the synchrotron radiation of the accelerated electrons. For an electron energy of 500 MeV, the circulating electron beam, according to Korolev,<sup>[5]</sup> is approximately elliptical in shape with a horizontal axis of 10 mm and a vertical axis of 3 mm. In our case the laser produces up to 0.5 joule of radiation in a pulse, which amounts to  $1.5 \times 10^{18}$  photons with  $\lambda = 6943 \text{ \AA}$ . The FIAN 600 MeV synchrotron accelerates in one cycle an average of  $10^{10}$  electrons (equilibrium orbit radius 2 m). The effective number of electrons participating in the interaction for the optical system and collimator dimensions chosen is of the order of  $10^7$  particles. Thus, for optimum overlap of the colliding photon and electron beams, a scattering cross section of the order of  $6 \times 10^{-25} \text{ cm}^2$ , and an electron energy of 550 MeV, we should expect the appearance of about 10 scattered photons per acceleration cycle with a maximum energy of the order of 7 MeV. The apparatus records  $\gamma$ -rays dissipating 5-9 MeV in the crystal.

Because of the incomplete overlap of the interacting beams due to the difference in their shapes (circle and ellipse), losses of laser light in the optical elements, absorption of  $\gamma$  rays in air and other materials in the path to the counter, and poor  $\gamma$ -ray detection efficiency in the scintillator, the counting rate can drop almost to 0.5 photon per acceleration cycle.

A statistical analysis showed that, in the measurements carried out under the conditions described, an average of  $1.06 \pm 0.08$  photons per acceleration cycle were observed (the number of events observed was 201). The background in the absence of laser light was  $0.64 \pm 0.006$  photon per cycle; no pickup from turning on the laser was re-

corded by the electronic equipment.

Thus, the number of  $\gamma$  rays which can be identified as scattered from electrons is  $0.42 \pm 0.08$  per acceleration cycle and per laser pulse.

On the basis of the experimental result obtained, we can state that we have detected the Compton scattering of 1.79 eV laser photons on 550 MeV relativistic electrons in a head-on collision of the beams.

Increase in the number of scattered  $\gamma$  rays by tens or hundreds of times by use of a more powerful laser (up to 20-30 joules), transfer of the interaction region to a straight section of the electron orbit, and incorporation of the interaction region in the resonant optical path of the laser<sup>[2]</sup> promises to diminish the main experimental difficulty - adjustment of the apparatus to achieve proper collision of the beams - and to make possible measurement of the energy and angular characteristics of the beam.

The authors are deeply grateful to Doctor of Physical-Mathematical Sciences A. M. Baldin for

his initiative in organizing this study and for his attention to the work. The authors also thank Professor F. A. Korolev and Professor V. A. Petukhov for their unceasing aid in this work and for helpful discussions.

<sup>1</sup>A. I. Akhiezer and V. B. Berestetskiĭ, *Kvantovaya elektrodinamika (Quantum Electrodynamics)*, 2d. ed., Gostekhizdat, 1959, Sec. 28.

<sup>2</sup>R. H. Milburn, *Phys. Rev. Letters* 10, 75 (1963).

<sup>3</sup>F. R. Arutyunyan and V. A. Tumanyan, *JETP* 44, 2100 (1963). *Soviet Phys. JETP* 17, 1412 (1963).

<sup>4</sup>Arutyunyan, Gol'dman, and Tumanyan, *JETP* 45, 312 (1963), *Soviet Phys. JETP* 18, 218 (1964).

<sup>5</sup>Korolev, Ershov, and Kulikov, *JETP* 40, 1644 (1961), *Soviet Phys. JETP* 13, 1158 (1961).

Translated by C. S. Robinson  
223

## ION THRESHOLD ENERGY FOR A TWO-STREAM ION INSTABILITY

M. D. GABOVICH and G. S. KIRICHENKO

Submitted to JETP editor July 2, 1964

J. Exptl. Theoret. Physics (U.S.S.R.) 47, 1594-1595 (October, 1964)

THE relative motion of an ion beam and a plasma or plasma streams can lead to a two-stream ion instability<sup>[1,2]</sup> if certain relations are satisfied between the electron thermal energy and the energy of the directed ion motion. This instability has been observed experimentally in a number of investigations.<sup>[3-5]</sup>

An ion beam with ion energies greater than the thermal energy of the ions in the plasma through which it passes can excite oscillations. As the beam energy increases further the system becomes stable. According to the hydrodynamic theory the threshold energy is a weak function of the ratio of the ion density in the beam to the ion density in the plasma and is given by  $\epsilon_{th} = 2\gamma kT_e$  when these two quantities are equal. The kinetic analysis<sup>[2]</sup> yields the relation  $\epsilon_{th} \approx 3kT_e$ .

By transmitting an ion beam (with a current of order 1 ma) through a plasma formed in various

gases one can observe the excitation of oscillations by the ion beam at various electron temperatures and verify this prediction of the theory over a relatively wide range of electron temperature.

The curve showing the dependence of oscillation amplitude on ion energy goes through a maximum value. The threshold energy is determined by the maximum of these curves, which precedes a more or less sharp reduction in oscillation amplitude. The function  $\epsilon_{th}(T_e)$  obtained in this way is shown in the figure. It is evident that there is a proportionality between the ion threshold energy and the electron temperature, as follows from the theory. The quantitative agreement between theory and experiment that is obtained with

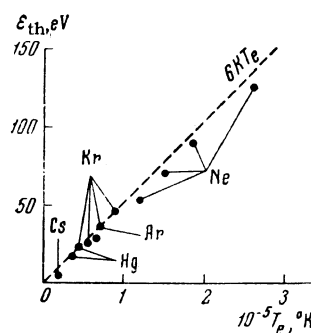


FIG. 1